Proc. NIPR Symp. Polar Meteorol. Glaciol., 9, 76–86, 1995

RELATION BETWEEN SURFACE ICE FLOW AND ANISOTROPIC INTERNAL RADIO-ECHOES IN THE EAST QUEEN MAUD LAND ICE SHEET, ANTARCTICA

Hideo MAENO[1], Shuji FUJITA[2], Kokichi KAMIYAMA[3], Hideaki MOTOYAMA[3], Teruo FURUKAWA[3] and Seiho URATSUKA[1]

[1]*Communications Research Laboratory, Ministry of Posts and Telecommunications, 2–1, Nukui-kitamachi 4-chome, Koganei-shi, Tokyo 184*
[2]*Department of Applied Physics, Faculty of Engineering, Hokkaido University, Kita-13, Nishi-8, Kita-ku, Sapporo 060*
[3]*National Institute of Polar Research, 9–10, Kaga 1-chome, Itabashi-ku, Tokyo 173*

Abstract: The polarimetric characteristics of radio-echoes reflected in the Antarctic ice sheet (internal radio-echoes) were investigated to clarify the relationship between the preferred orientation of ice crystals and the polarization of electromagnetic waves. The radio-echo sounding was carried out with an 179 MHz radio-echo sounder at 14 different sites along the oversnow traverse route from Syowa Station to Dome Fuji in the distance of about 1000 km roughly along the flow line in the Shirase Glacier drainage. The A-scope data were obtained at each site from 16 different orientations of the transmitting and receiving antennae, kept parallel to one another. The internal radio-echoes reflected were found to be strongly polarized. In addition, a good correlation was found between the measured surface flow vectors and the orientation dependence of the attenuation. That is, the antennae orientations that give the maximum attenuation are always parallel to the flow line. Moreover, the differences between the maximum and minimum values of the attenuation coefficient at each site are proportional to the flow velocity. These results suggest that polarimetric radio-echo sounding (PRES) is applicable to a technique as follows: 1) to measure approximate flow vector; 2) to investigate deeper layers by orienting the antennae perpendicular to the flow line; and 3) to investigate the dynamics around the summit of the ice sheet.

1. Introduction

The importance of monitoring the global environment has grown in recent years. Many studies aiming at solving global environmental problems are being carried out in the Arctic and Antarctic regions, since the polar regions play very important roles in the global climate. Therefore, understanding of the changes in the Antarctic ice sheet, *i.e.*, about its growth and retreat, its structure and inherent dynamical properties, is essential for understanding global climate change.

Radio-echo sounding (RES) of ice sheets is a powerful technique to investigate their internal structure and thickness. The radio-echo sounders have been operated at frequencies between ten and several hundred MHz (*e.g.* ROBIN *et al.*, 1969; BOGORODSKY *et al.*, 1985). Since radio-echoes are caused by changes in the complex permittivity of the layers that comprise the ice sheets, knowledge of the dielectric properties of ice is

a key to interpret the internal radio-echoes from within the ice sheet. In addition to the earlier knowledge of dielectric properties (reviewed in EVANS, 1965; WARREN, 1984), several other properties have been clarified recently (FUJITA *et al.*, 1992, 1993; MOORE and FUJITA, 1993). Due to this progress, the RES technique has remarkably gained in potential to investigate internal structures of ice sheets using internal radio-echoes. It can be summarized in two parts as follows: 1) we can investigate the preferred orientation of ice crystals (crystal orientation fabrics) in the ice sheet by analyzing the polarization state of internal radio-echoes (HARGREAVES, 1977, 1978; FUJITA and MAE, 1993; LIU *et al.*, 1994); and 2) we can investigate the causes of internal reflections using multi-frequency RES (FUJITA and MAE, 1994). Particularly, about the former technique, HARGREAVES (1977, 1978) established the theoretical basis. The discovery of the dielectric anisotropy of ice crystals (FUJITA *et al.*, 1993) has made concrete quantitative discussions possible.

We tested this technique in order to investigate the dynamical condition in the Antarctic ice sheet along a route from coast to summit. In this study, we observed the polarization state of internal radio-echoes with an 179-MHz radio-echo sounder, and then compared it with the flow velocity vector measured using the GPS at each observational site. RES observations were carried out along the Syowa Station–Mizuho Station–Dome Fuji traverse route, in the East Queen Maud Land in East Antarctica, by the 33rd Japanese Antarctic Research Expedition (JARE-33, November 1991–March 1993) (MAENO *et al.*, 1994). This research is a contribution to the Deep Ice Coring Project at Dome Fuji. Flow velocity vectors along the route were measured by MOTOYAMA *et al.* (1995).

In East Queen Maud Land, YOSHIDA *et al.* (1987) first carried out the polarimetric RES (hereafter PRES) in 1984 at Mizuho Station using the 179-MHz radio-echo sounder. They detected the birefringence of the ice sheet, and found that the strength of the internal radio-echoes increased when the two parallel antennae azimuths were parallel or perpendicular to the observed flow line. Since the flow line was parallel to the tensile principal strain of the ice sheet, it was proposed that the crystal orientation fabrics might determine the birefringence of the ice sheets. FUJITA and MAE (1993) extended the discussion. They confirmed that the ice sheet at Mizuho Station was a uniaxially birefringent medium, and explained the relation between the polarized internal radio-echoes and the crystal orientation fabrics in the ice sheet. In this study, we have expanded the measurement up to 14 sites along the route. Through the preliminary analysis, we found a remarkable empirical relation between the polarization state of the internal radio-echoes and the flow velocity vector at each site.

2. Experiments

2.1. Radio-echo sounder and antennae system

The 179-MHz radio-echo sounder used in the experiments is composed of a transmitter, a receiver, a recorder and two antennae. All instruments except the antennae that were mounted on the roof of the oversnow vehicle were installed inside the vehicle. Major characteristics of the sounder are shown in Table 1, and details of the system are described in MAENO *et al.* (1994). A pulse width of 1 μs was used in most

Table 1. Major characteristics of the 179-MHz radio-echo sounder system.

Transmitter	Frequency	179 MHz
	Peak power	1 kW
	Pulse width	60/250/1000 ns
	Resolution in air	9/37.5/150 m
	in ice[1]	5.1/21.4/85.5 m
	Repetition period	1 ms
Receiver	Sensitivity[2]	−110 dBm
	Band width	14/4/1 MHz
	Noise figure	<1 dB
Antenna	Type	8-element Yagi, 2 stack×2
	Gain	16.5 dBi
	Beam width	20 degrees (in air)
Recording	Digital	3.5-inch floppy disk
		2048 byte per minute
		256 times averaging

[1] Refractive index of 1.78 is assumed.
[2] Receiver bandwidth is 4 MHz.

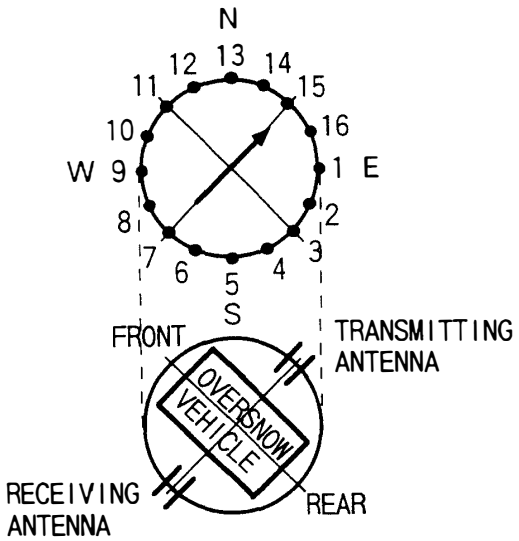

Fig. 1. Positions of the two antennae seen from the oversnow vehicle and the orientation of the linearly-polarized two-stacked Yagi antennae (lower diagram). In the upper diagram, geographical orientation is defined by numbers 1 to 16. This example shows that the oversnow vehicle was pointing NW, hence the two antennae are oriented SW-NE. In the analysis of the data, the direction of the transmitting antenna was considered (see the arrow in the upper diagram).

measurements. The recording parameters such as the range and the averaging number were selected depending on the purpose of the measurements and on the estimated ice thickness. We stacked data at least 256 times for averaging.

The locations of the antennae and the oversnow vehicle are schematically shown in Fig. 1. Two 2-stacked 8-element Yagi antennae were used: one on the right side of the vehicle for transmitting and the other on the left side for receiving. The radio waves were transmitted toward the ice sheet at the nadir. The polarization plane containing the electric field vector of the transmitted wave was always in the orientation of the two antennae on the vehicle (see Fig. 1).

2.2. Method of polarimetric RES

Since the polarization planes of both the transmitting and receiving antennae are in the same orientation, only the co-polarized return waves were received. The A-scope image (the vertical profiles of the internal radio-echoes) in 16 different antennae azimuths (*i.e.* polarization plane) were measured. In each observation, the polarization plane was changed by changing the direction of the vehicle. The definitions of direction are also shown in Fig. 1. Direction No. 1 was chosen as east and the other directions Nos. 2, 3, ..., 16 were defined from No. 1 with clockwise increments of 22.5°. The direction of each number indicates the direction of the transmitting antenna seen from the vehicle. Each direction corresponds to the orientation of the polarization plane. In

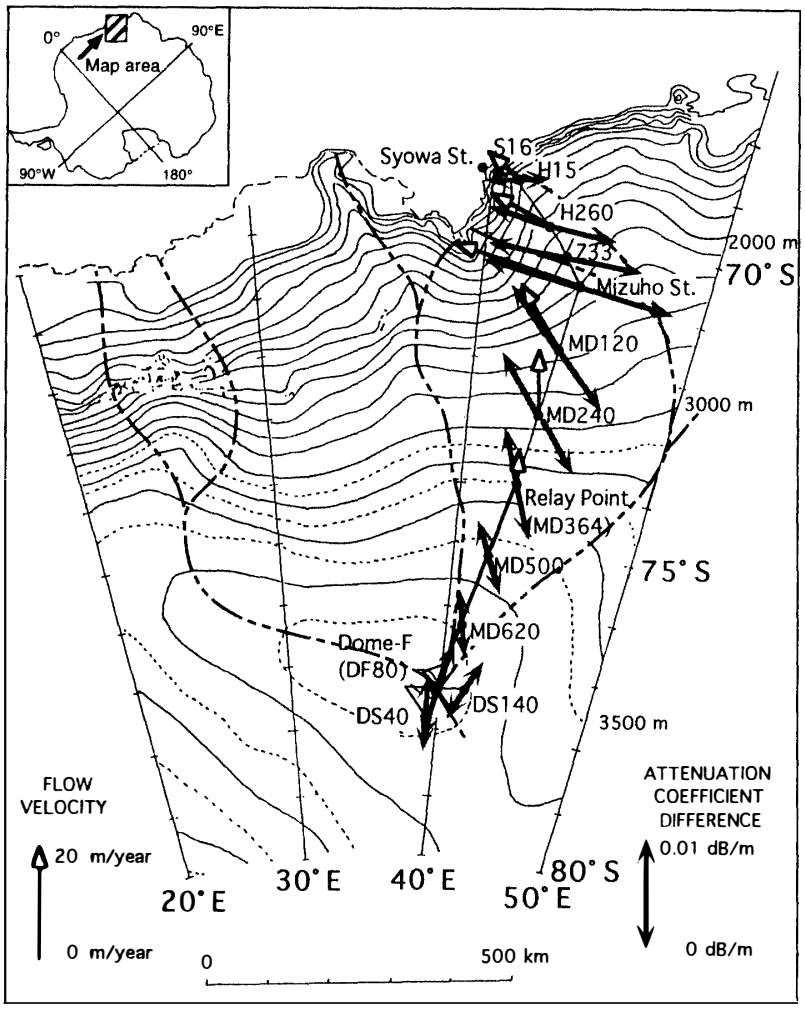

*Fig. 2. Map of the ice sheet in the region of the Shirase Glacier Drainage Basin and Dome Fuji. Fourteen observational sites are indicated, with the flow velocity vectors measured by the GPS differential method (*Motoyama *et al., 1995) and with the results of the polarimetric RES (PRES) measurement. The orientation at which the attenuation coefficient of the internal radio-echo was a maximum is shown by an arrow at each site. The length of the arrow indicates the magnitude of the ACD (see the text for the definition of ACD).*

the measurement, geographical orientations were determined by using a magnetic compass and an optical fiber gyroscope.

2.3. Observational sites

Fourteen observational sites are shown on the map numbered in Fig. 2. They are located roughly along the flow line from the summit of the ice sheet (Dome Fuji), through Mizuho Station, to the coast line (Syowa Station), in the Shirase glacier drainage basin. A typical distance between adjacent sites was about 120 km. The details of the locations of the sites are also shown in Table 2. In the drainage basin, ice flows divergently in the up-stream area and convergently in the lower-stream area, as can be seen in the map in Fig. 2.

Among the sites listed in Table 2, we analyzed the data except at site S16 and site D04. The data from the former site were excluded because the setting parameters of the RES observation were different from the others. The data from the latter site were excluded because of malfunction of the receiver.

Table 2. List of observation sites.

Site	Date (1992)	Lat.	Lon.	Elevation (m)	Thickness (m)
DS40	30 Oct.	77° 44′	39° 07′	3770	2260
DS140	3 Nov.	77° 21′	41° 18′	3771	2970
DF80	3 Nov.	77° 22′	39° 36′	3807	2800
D04	13 Nov.	77° 21′	39° 34′	3807	2750
MD620	21 Nov.	76° 18′	40° 49′	3722	3130
MD500	25 Nov.	75° 13′	42° 00′	3618	3300
MD364	28 Nov.	74° 00′	42° 59′	3353	2780
MD240	4 Dec.	72° 53′	43° 28′	3001	1890
MD120	8 Dec.	71° 49′	43° 53′	2600	2500
Mizuho	12 Dec.	70° 42′	44° 16′	2250	2060
Z33	15 Dec.	70° 16′	43° 34′	2065	1540
H260	16 Dec.	69° 52′	42° 41′	1776	1760
H15	20 Dec.	69° 04′	40° 46′	1050	1030
S16	20 Dec.	69° 01′	40° 03′	591	350

3. Results

3.1. Anisotropic internal radio-echoes

Figure 3 shows A-scope images in 16 different measurement directions obtained at three sites: (a) DF80 (Dome Fuji), (b) MD364 (Relay Point), and (c) Mizuho Station, respectively. The results at these three sites are chosen to show general tendencies. Although we describe several features found only in the three examples below, all these features were found in the result at every site. All three examples clearly indicate that the reflected signal strength has a strong dependency on orientation of polarization. Both the internal reflections and the reflections from the bedrock have this dependence. In addition, decrease of return power with increasing depth, *i.e.* attenuation coefficients, also have strong dependency on orientation of polarization. Due to this strong depen-

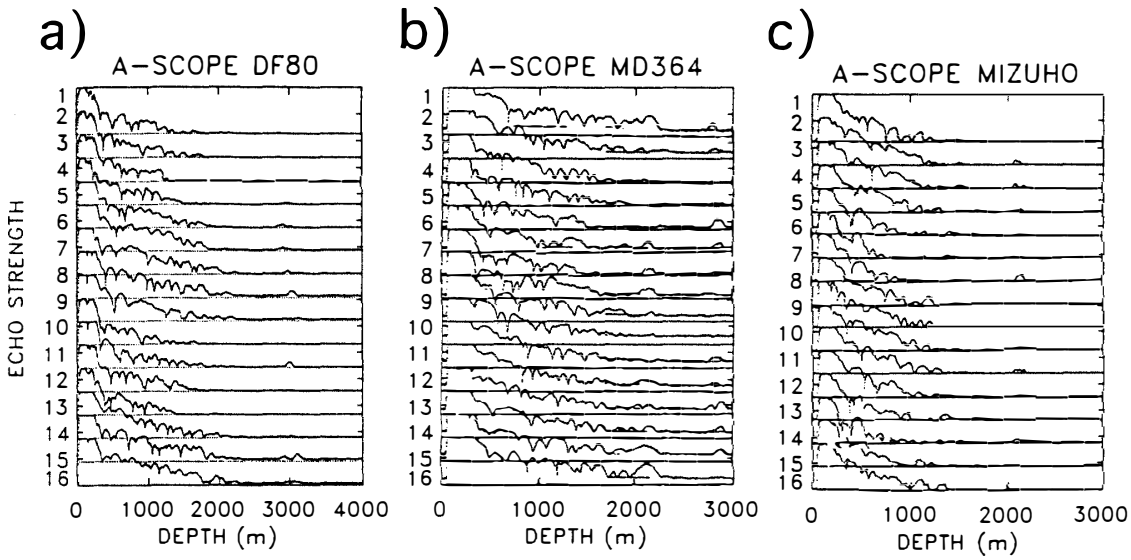

Fig. 3. Examples of A-scope images in 16 different measurement directions obtained at three sites: (a) DF80 (Dome Fuji), (b) MD364, and (c) Mizuho Station. Note that the return signal up to about 200 m was saturated by the transmitting pulse. The power received from the internal layers deeper than about 2000 m was below the detection level. The return signal from the bedrock surface was much stronger than the signal from an internal layer in the ice sheet at the same depth. The echoes from the bedrock appeared clearly even when the depth was more than 2800 m.

dency on orientation of polarization, one can see that the penetration depth of the radio-waves has strong dependency on orientation of polarization in Fig. 3.

These three examples indicate also that the penetration depth increases with increasing distance from the coast line. At Mizuho Station, the detection limit of the internal radio-echoes is around 1500 m in depth. In contrast, it is around 2000 m at sites in the inland region, *i.e.* at MD364 and at DF80. This tendency has already been shown by MAENO *et al.* (1994) from the analyses of returned power from the bedrock, along the same route from the coast to the summit. Regional difference of radio waves attenuation has been discussed also by OHMAE *et al.* (1984) using a 60-MHz radar data collected at Mizuho Plateau. They also pointed out that values of attenuation coefficient become smaller with increasing surface elevation of the ice sheet.

Note that the results at Mizuho Station have the same tendency as was observed by YOSHIDA *et al.* (1987). The important common features between the two observations are: 1) strong reflections were observed when the antennae were oriented parallel or perpendicular to the flow line (see bedrock echo 3, 7, 11 and 14 in Fig. 3c); and 2) a strong internal reflection was observed at around 500 m depth where a layer containing visible volcanic ash was found in the 700 m Mizuho ice core (FUJII and WATANABE, 1988). These common features between the two measurements carried out using different systems in different years (1984 and 1991–1993, respectively) prove both the reproducibility and the reliability of the two measurements. Feature 1) is evidence that birefringence occurred in the ice sheet (FUJITA and MAE, 1993).

3.2. Orientation dependence of attenuation coefficients

Although earlier studies (YOSHIDA *et al.*, 1987; FUJITA and MAE, 1993) analyzed

the orientation dependence of the signal strength returned from each depth, in this study we particularly analyzed the attenuation of the signals with depth. Figure 4 shows an example of an A-scope image after geometrical corrections for radar beam expansion with distance (inversely proportional to the square of distance from the radar to the target). Because we can assume that the volume scattering cross section is constant, the image shows purely attenuation of the radio waves in the ice sheet. The attenuation

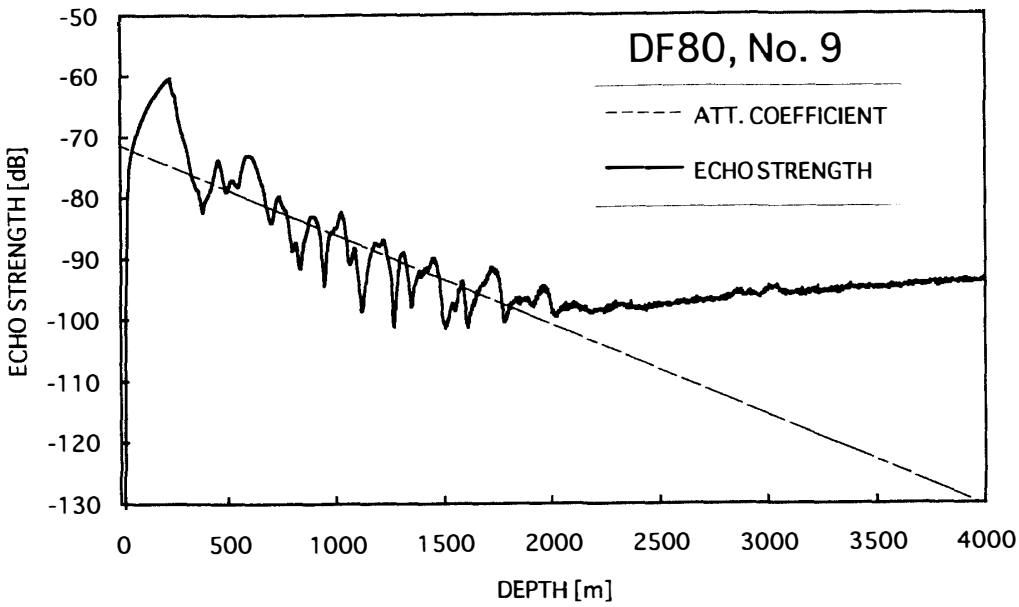

Fig. 4. An example of the A-scope image after the geometrical corrections. The dashed line is a regression line used for the calculation of the attenuation coefficient.

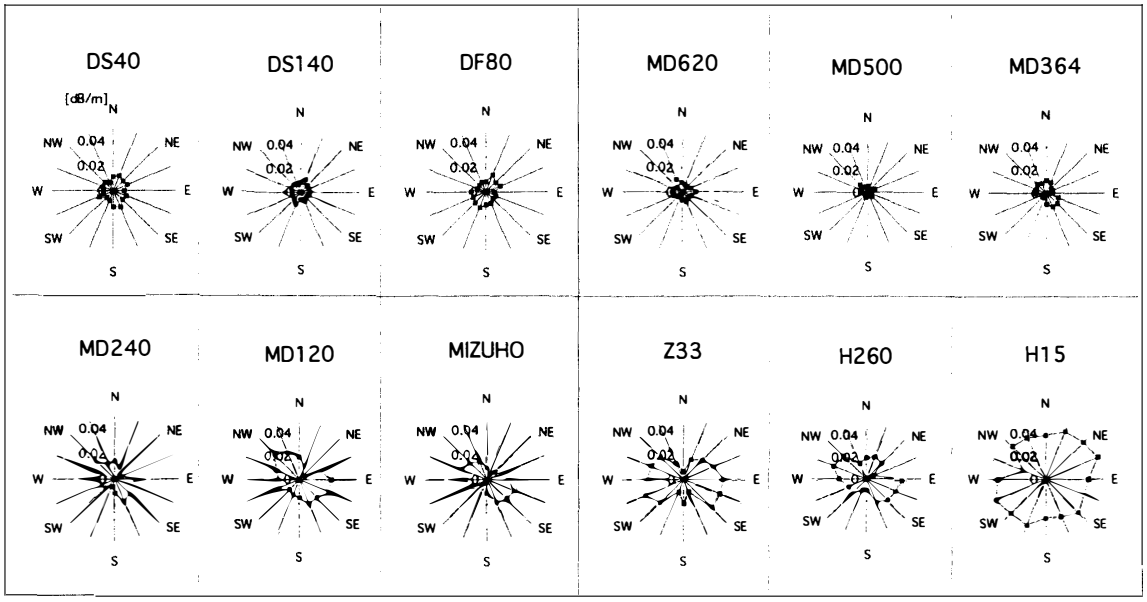

Fig. 5. The attenuation coefficients as a function of the antennae orientation at all 12 sites. In each diagram, we can clearly see a bi-polar anisotropy in the coefficient with respect to the antennas orientation.

coefficient for each A-scope image was calculated by a least-squares fitting in the range from 300 m to a depth at which the return signal almost disappears but is still larger than noise level, as in the example in Fig. 4. With this procedure, we derived attenuation coefficients of radio-waves as a function of antennae orientation, *i.e.* polarization plane orientation.

Figure 5 shows the attenuation coefficients as a function of the antennae orientation at 12 sites. In each diagram, we can clearly see a bi-polar anisotropy in the coefficient with respect to the antennae orientation. In addition, the attenuation coefficients are a maximum when the antenna orientation is parallel to the flow vector at each site and a minimum when the antenna orientation is perpendicular to the flow vector. For example, at Mizuho Station, the flow vector from ESE to WNW (NISHIO *et al.*, 1989; MOTOYAMA *et al.*, 1995) corresponds to the orientation at which the maximum attenuation coefficient was observed. The same relationship was found at other sites. This will be discussed later. It should be noted that in Fig. 5 the attenuation coefficients at sites close to the coast are larger but in the interior region they are smaller, as was also seen in Fig. 3.

4. Discussion

4.1. Empirical relation between the flow velocity vector and the anisotropic radio-echo

We tentatively compared the orientation dependence of the attenuation coefficients with the flow velocity vectors measured at each site by a GPS differential method (MOTOYAMA *et al.*, 1995). We define the difference in attenuation coefficients between the average of the maximum pair in an orientation and the average of the minimum pair in the orientation perpendicular to the former pair, as the ACD (Attenuation Coefficient Difference). We define them in this way because the maximum values can be more easily defined than the minimum values. The direction in which the maximum attenuation

Table 3. List of flow vectors and factors of anisotropic radio-echoes.

Site	Flow vector		Orientation at which the attenuation was the maximum and the ACD		
	Direction (°)	Velocity (m/year)	Orientation (°)		ACD (dB/m)
DS40			0–90	(N-S)	0.0039
DS140			22.5–202.5	(NNE-SSW)	0.0032
DF80			22.5–202.5	(NNE-SSW)	0.0065
D04					
MD620			157.5–337.5	(NNW-SSE)	0.0024
MD500			135–315	(NW-SE)	0.0046
MD364	359	4.1	157.5–337.5	(NNW-SSE)	0.0064
MD240	354	8.0	135–315	(NW-SE)	0.0103
MD120	332	17.8	135–315	(NW-SE)	0.0179
Mizuho	297	22.2	112.5–292.5	(WNN-EWE)	0.0188
Z33			90–270	(W-E)	0.0179
H260	306	14.5	90–270	(W-E)	0.0139
H15	300	6.7	90–270	(W-E)	0.0030
S16	288	5.2			

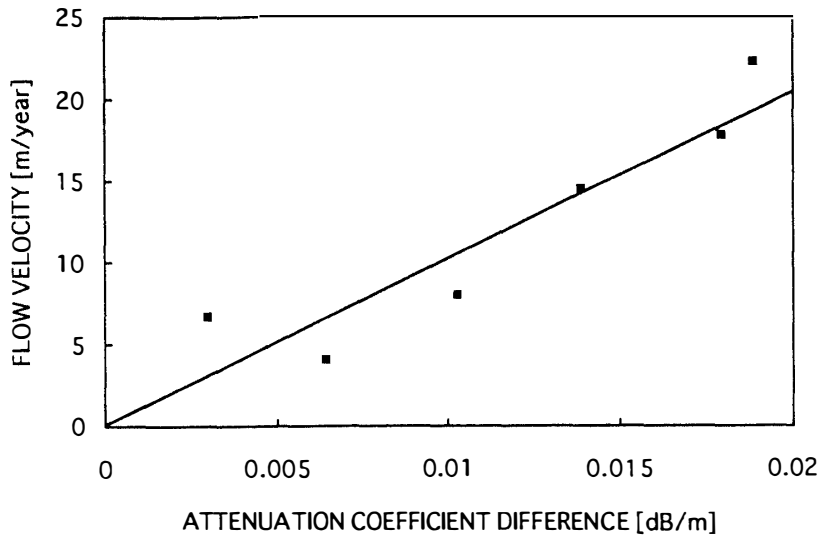

Fig. 6. The relationship between the measured flow velocities and the attenuation coefficient differences.

occurred was determined at each site and then the ACD was calculated. The results are shown in Table 3 and Fig. 2. The flow velocity vectors measured are also shown in Table 3 and Fig. 2. It was found that the direction of the flow vector appears to coincide with the orientation at which the maximum attenuation occurred. In addition, the ACD and the magnitudes of flow velocity vectors were proportional to each other. The proportional relation between them is indicated empirically as 1.0×10^{-3} (dB year m^{-2}) in Fig. 6. It is noticeable that the flow vector tends to deviate clockwise by 10–40° from the orientations at which the maximum attenuation was observed.

4.2. Physical mechanism

Although the relation between the ACD and the flow velocity is empirical, there is a linking physical mechanism between them. The orientation dependence of the attenuation coefficients is clearly caused by birefringence due to crystal orientation fabrics (FUJITA and MAE, 1993; HARGREAVES, 1977, 1978). Since the crystal orientation fabrics are formed due to strain in the ice (*e.g.* AZUMA and HIGASHI, 1986; AZUMA, 1994, 1995), strain creates the birefringence and hence the ACD. The strain was accumulated in the ice along particle paths of ice at each depth. On the other hand, the flow velocity vector is also created by strain in the ice. The vector is the integral of the horizontal shear strain rate from the surface to the bottom and it is also the integral of the normal tensile strain rate along the flow line from the summit to each site. Therefore since both are the results of integration of strain in the ice sheet, they are highly correlated. Although the discussion above is a qualitative one at present, it should be discussed quantitatively in the future considering the development of crystal orientation fabrics in the ice sheet (AZUMA and HIGASHI, 1986; AZUMA, 1994, 1995) and the propagation of the electromagnetic waves in anisotropic ice (HARGREAVES, 1977, 1978). Note that the difference in orientation between the flow vector and the orientation at which the maximum attenuation coefficients were found, 10–40°, may be caused by vertical shear strain in the ice. This implies that the flow velocity and the

principal axis of the strain do not exactly correspond with each other at each site.

4.3. Suggestion for future RES

Based on the results of this study, new RES technique can be suggested for the future glaciological research in the Antarctica. The first one can estimate the flow direction and flow velocities from the orientation dependence of the attenuation coefficients. The advantage of this technique is that one does not need to wait to obtain the approximate velocity data, unlike the GPS differential method. The second one can detect a stronger bedrock echo if both the transmitting and the receiving antennae are oriented perpendicular to the flow direction. To detect deep bedrock echoes and internal radio-echoes at deeper layers, this will be a convenient technique. The third one can use PRES to find a site at which there is no strain in the horizontal plane around the summit of the ice sheet. Then one should find a site at which the ACD is zero. This will be useful for the site selection for deep ice-coring at the summit and for investigating the dynamical condition around the summit.

5. Concluding Remarks

Preliminary results of PRES in the Antarctic ice sheet were presented. We found that both the signal strength of the internal radio-echoes and the attenuation coefficients strongly depend on the orientation of the antennae azimuth, *i.e.* orientation of the polarization plane. The orientation dependence of the attenuation coefficients showed a clear bipolar pattern. In addition, the orientations in which the attenuation coefficient was maximum were always approximately parallel to the flow direction of the ice sheet.

Moreover, the ACD was proportional to the flow velocity. The ACD increases linearly with increasing velocity at a rate of 1.0×10^{-3} (dB year m^{-2}). The empirical relation can be qualitatively explained as the result of cumulative strain in the ice sheet. This is because the flow velocity is the integration of the strain in the ice sheet and the crystal orientation fabrics, which causes the birefringence, and is also formed by the strain integrated along the particle paths. This should be discussed quantitatively in the future. Based on the results of our experiment, a new PRES technique was suggested for future glaciological research. These techniques are summarized as follows: 1) to measure approximate flow vectors *in-situ*; 2) to investigate deep layers by orienting the antennae perpendicular to the flow direction; and 3) to investigate the dynamical condition around the summit of the ice sheet, particularly to find a site at which there is no horizontal shear strain. PRES will be a powerful technique to obtain information for understanding the internal structure of the ice sheet and its dynamical properties.

Acknowledgments

We are grateful to Prof. M. FUKUCHI, the leader of the winter party, and the members of the JARE-33 for their cooperation in the field work. We are also grateful to Prof. O. WATANABE from the National Institute of Polar Research, Prof. F. NISHIO from the Hokkaido University of Education and Prof. R. NARUSE from the Institute of Low Temperature Science, Hokkaido University for their support in this study. This

work is a contribution to the Deep Ice Coring Project at Dome Fuji.

References

AZUMA, N. (1994): A flow law for anisotropic ice and its application to ice sheet. Earth Planet. Sci. Lett., **128**, 601–614.

AZUMA, N. (1995): A flow law for anisotropic policrystalline under uniaxial compressive deformation. Cold Reg. Sci. Technol., **23**, 137–147.

AZUMA, N. and HIGASHI, A. (1985): Formation processes of ice fabric pattern in ice sheets. Ann. Glaciol., **6**, 130–134.

BOGORODSKY, V.V., BENTLEY, C.R. and GUDMANDSEN, P.E. (1985): Radioglaciology. Dordrecht, D. Reidel, 254p.

EVANS, S. (1965): Dielectric properties of ice and snow-A review. J. Glaciol., **5**, 773–792.

FUJII, Y. and WATANABE, O. (1988): Microparticle concentration and electrical conductivity of a 700 m ice core from Mizuho Station, Antarctica. Ann. Glaciol., **10**, 38–42.

FUJITA, S. and MAE, S. (1993): Relation between ice sheet internal radio-echo reflections and ice fabric at Mizuho Station, Antarctica. Ann. Glaciol., **17**, 269–275.

FUJITA, S. and MAE, S. (1994): Causes and nature of ice-sheet radio-echo internal reflections estimated from the dielectric properties of ice. Ann. Glaciol., **20**, 80–86.

FUJITA, S., SHIRAISHI, M. and MAE, S. (1992): Measurement on the dielectric properties of acid-doped ice at 9.7 GHz. IEEE Trans. Geosci. Remote Sensing, **30**, 799–803.

FUJITA, S., MAE, S. and MATSUOKA, T. (1993): Dielectric anisotropy in ice Ih at 9.7 GHz. Ann. Glaciol., **17**, 276–280.

HARGREAVES N.D. (1977): The polarization of radio signals in the radio echo sounding of ice sheets. J. Phys. D, **10**, 1285–1304.

HARGREAVES, N.D. (1978): The radio-frequency birefringence of polar ice. J. Glaciol., **21**, 301–313.

LIU, C., BENTLEY, C.R. and LOAD, N.E. (1994): *c* axis from radar depolarization experiments at Upstream B Camp, Antarctica, in 1991–92. Ann. Glaciol., **20**, 169–176.

MAENO, H., KAMIYAMA, K., FURUKAWA, T., WATANABE, O., NARUSE, R., OKAMOTO, K., SUITZ, T. and URATSUKA, S. (1994): Using a mobile radio echo sounder to measure bedrock topography in East Queen Maud Land, Antarctica. Proc. NIPR Symp. Polar Meteorol. Glaciol., **8**,149–160.

MOORE, J.C. and FUJITA, S. (1993): Dielectric properties of ice containing acid and salt impurity at microwave and low frequencies. J. Geophys. Res., **98**, 9769–9780.

MOTOYAMA, H., ENOMOTO, H., FURUKAWA, T., KAMIYAMA, K., SHOJI, H., SHIRAIWA, T., WATANABE, K., NAMASU, K. and IKEDA, H. (1995): Preliminary study of ice flow observations along traverse routes from coast to Dome Fuji, East Antarctica by differential GPS method. Nankyoku Shiryô (Antarct. Rec.), **39**, 94–98.

NISHIO, F., MAE, S., OHMAE, H., TAKAHASHI, S., NAKAWO, M. and KAWADA, K. (1989): Dynamical behavior of the ice sheet in Mizuho Plateau, East Antarctica. Proc. NIPR Symp. Polar Meteorol. Glaciol., **2**, 97–104.

OHMAE, H., NISHIO, F., ISHIKAWA, M., KATSUSHIMA, T. and TAKAHASHI, S. (1984): Regional difference of attenuation of radio waves within Antarctic ice sheet. Mem. Natl Inst. Polar Res., Spec. Issue, **34**, 152–159.

ROBIN, G. de Q., EVANS, S. and BAILEY, J.T. (1969): Interpretation of radio echo sounding in polar ice sheets. Philos. Trans. R. Soc. London, Ser. A, **265**, 437–505.

WARREN, S.G. (1984): Optical constants of ice from the ultraviolet to the microwave. Appl. Optics, **23**, 1206–1225.

YOSHIDA, M., YAMASHITA, K. and MAE, S. (1987): Bottom topography and internal layers in East Droning Maud Land, East Antarctica, from 179 MHz radio echo-sounding. Ann. Glaciol., **9**, 221–224.

(Received December 27, 1994; Revised manuscript received June 2, 1995)